Supplemental Data

The Nuclear Orphan Receptor NR2F6 Suppresses Lymphocyte Activation and T Helper 17-Dependent Autoimmunity

Natascha Hermann-Kleiter, Thomas Gruber, Christina Lutz-Nicoladoni, Nikolaus Thuille, Friedrich Fresser, Verena Labi, Natalia Schiefermeier, Marei Warnecke, Lukas Huber, Andreas Villunger, Gregor Eichele, Sandra Kaminski, and Gottfried Baier

Supplemental Experimental Procedures

Analysis of proliferation responses

Antibody- and alloantigen-induced proliferation was measured after 64 hrs by [^{3}H]thymidine incorporation during the last 16 hrs using a Matrix 96 direct β counter system. $CD4^+$ and $CD8^+$ T cells were negatively selected by magnetic cell sorting (Miltenyi Biotec). For anti-CD3 stimulations, T cells ($5x10^5$) in 200 µl proliferation medium (RPMI supplemented with 10% FCS, 2 mM L-glutamine and 50 units ml^{-1} penicillin/streptomycin) were added to plates precoated with anti-CD3 antibody (clone 2C11, 10 µg ml^{-1}) in duplicates. Where indicated soluble anti-CD28 (1 µg ml^{-1}; BD Bioscience) was added. Splenic B cells were purified by depletion of non-B cells on MACS columns (Miltenyi Biotec) with anti-CD43 Abs coupled to magnetic beads (Miltenyi Biotec). B cells were stimulated with 1.2 or 2.4 µg ml^{-1} goat anti-mouse IgM $F(ab´)_2$ (Dianova) in combination with 25 U ml^{-1} recombinant mouse IL-4 (Roche).

Flow cytometry

Single-cell suspensions of spleen, lymph node, thymus or bone marrow were prepared and incubated for 30 min on ice in staining buffer (PBS containing 2% FCS and 0.2% NaN_3) together with FITC, PE, APC or biotinylated antibody conjugates. Surface marker expression was analyzed using a FACS Calibur cytometer (BD Biosciences) together with CellQuestPro

software. Abs against murine CD3, CD4, and CD8 were obtained from Caltag Laboratories; CD28, CD69, CD44, CD25, CD62L, ICOS, TCR, Vβ8, CD19, B220, IgM, IgD, CD43, CD5, CD21, CD23, Ger1, Mac1, Thy1 and CD19 were obtained from BD Pharmingen, FOXP3, B220 and CD21/CD35 from eBioscience. Streptavidin–RPE (Dako) was used to stain biotinylated mAbs.

Detection of autoantibodies in mouse serum on rat liver sections and with ELISA

Slides precoated with rat liver sections were used to evaluate the presence of ANA in mouse blood serum using an Alexa Fluor 488 goat anti-mouse IgG1 antibody (Molecular Probes). Measurement of autoantibodies against double-stranded DNA was performed by ELISA (α-Diagnostics). Results were expressed as absorbance at 450 nM.

Determination of serum immunoglobulin (Ig) levels

The concentration of different Ig subclasses in mouse sera was analyzed using isotype-specific antibodies using ELISA quantification kits for IgGa, IgG1, IgG, IgE and IgM obtained from Bethyl.

Apoptosis detection

Total splenocytes were used to generate activated T cell blasts using Con A (2 μg ml^{-1}) for 48 hrs, followed by IL-2 stimulation (100 U ml^{-1}) for additional 72 hrs. After 5 days, activated T cell blasts were washed twice; viable cells were enriched by Lympholyte^{TM} (Cedarlane) gradient centrifugation (viability >90%), and incubated in IMEM medium (10% FCS, 2 mM L-Glutamin and 50 U ml^{-1} Pen/Strep). Apoptosis sensitivity was challenged by different concentrations of anti-CD3 cross-linking Abs (clone 2C11) or cross-linked recombinant FasL (FasL 100 ng ml^{-1} & enhancer for FasL (at 1 μg ml^{-1}) to trigger activation-induced cell death. 8 hrs after apoptosis induction cells were harvested and then stained with annexin V-FITC

(Molecular Probes), anti CD4-PE and anti CD8-APC (Caltag). The percentage of apoptotic cells in each T cell subset was determined by FACS analysis using FACS Calibur (BD) and CellQuestPro software. Splenic B cells from *Nr2f6*$^{-/-}$ and *Nr2f6*$^{+/+}$ mice were purified in a FACSvantage sorter by negative cell sorting using following monoclonal antibodies: MI/70, anti–Mac-1 (eBioscience); Ter119, antierythroid cell surface marker (BD); T24.31.2, anti–Thy-1. B cells were cultured at an initial concentration of $5x10^5$ cells ml^{-1} in proliferation medium (RPMI supplemented with 10% FCS, 2 mM L-glutamine and 50 units ml^{-1} penicillin/streptomycin). For the induction of cell death anti-IgM F(ab) fragments (Jackson Immuno Research) were used. The percentages of viable cells in culture were determined by staining cell suspensions with propidium iodide plus annexin V-FITC (Molecular Probes).

Abbreviations

ANA anti nuclear antibody; AP-1 activating protein-1; CK1 casein kinase 1; COUP-TF chicken ovalbumin upstream promoter transcription factor; dsDNA double stranded DNA; EAE experimental autoimmune encephalomyelitis; EMSA electrophoretic mobility shift assay; FACS fluorescence-activated cell sorter; FOXP3 forkhead box P3; IFN-γ interferon γ; IL-2 interleukin-2; IL-17 interleukin-17; LTi lymphoid tissue inducer cells; i.p. intra-peritoneal; i.v. intra-venous; LXR liver x receptor; MOG Myelin oligodendrocyte protein; NF-AT nuclear factor of activated T cells; NF-κB nuclear factor of κB; NR nuclear receptor; NR2F6 nuclear receptor subfamily 2, group F, member 6; Nur77/NR4A1 nuclear receptor 77 subfamily 4, group A, member 1; OHT4-hydroxytamoxifen; PKB protein kinase B; PKC protein kinase C; PPAR peroxisome proliferator-activated receptor; RAR retinoic acid receptor; RORγ/NR1F3 retinoid-related orphan receptor γ/nuclear receptor subfamily 1, group F, member 3; RXR retinoid x receptor; SEB super antigen staphylococcal enterotoxin B; SEE super antigen staphylococcal enterotoxin E; TCR T cell receptor; and Th17 T helper cell subset producing IL-17.

Supplemental figure legends:

Figure S1: NR2F6 domain structure and mRNA levels in activated T cells

(A) Schematic of NR2F6 domain structure modified from (Giguere, 1999) showing the position of the putative PKC phosphorylation site at S83. (B) In mouse $CD3^+$ T cells, *Nr2f6* mRNA levels decreased after 4 h of stimulation with solid phase CD3 antibodies alone or in combination with co-stimulatory CD28. Mean of 3 independent experiments are shown and error bars represent standard error. Data were normalized to GAPDH.

Figure S2: NR2F6 interacts with PKCα and PKCθ and binds to its established TGACCT direct-repeat DNA motif in EMSA analysis

(A) Consistent with its identification as a PKC substrate, endogenous PKCα and PKCθ (but not PKB) bound to recombinant NR2F6 in GST-pull down assays. Such physical interaction occurred independently of T cell stimulation (CD3 ligation or PDBu treatment) and phosphorylation (Ser-83) status on NR2F6. One representative experiment out of three is shown. (B) EMSA analysis employing transient Jurkat transfections has confirmed that only a slight shift can be observed but supershifting mAb (directed against an epitope with amino acids 13-44 of NR2F6) reproducibly induced a conformational switch and/or increased avidity that stabilizes NR2F6 DNA-binding. We did not see this stabilization effect with non-specific antibody controls. The free probe does not shift with this NR2F6 mAb, as demonstrated in the GFP control transfections.

Figure S3: **Schematic cartoon of conditionally activated NR2F6-ER**, consisting of the NR2F6 DNA-binding domain (DBD) mutant fused to a mutated estrogen receptor ligand-binding domain (ER_{mut}-LBD). Exposure to OHT, the selective agonist of ER_{mut}-LBD within NR2F6-ER, strongly induced nuclear translocation of recombinant NR2F6-ER fusion mutant protein (not shown).

Figure S4: ***Nr2f6*$^{-/-}$ immature thymocytes are as sensitivity to negative selection as *Nr2f6*$^{+/+}$ controls**

Negative selection in double positive thymocytes ($CD4^+/CD8^+$) was induced by anti-CD3 antibody i.p. injection in *Nr2f6*$^{-/-}$ and *Nr2f6*$^{+/+}$ controls. FACS analysis after 24 h revealed no difference in thymocyte depletion between the genotypes (*Nr2f6*$^{+/+}$ n=3; *Nr2f6*$^{-/-}$ n=3). Means are shown; error bars represent standard error.

Figure S5: ***Nr2f6*$^{-/-}$ B cell development in the bone marrow is normal**

Cells derived from *Nr2f6*$^{-/-}$ and *Nr2f6*$^{+/+}$ controls were stained for pro-B cells ($B220^+CD43^+$), pre-B cells ($B220^+CD43^-IgM^-$), immature B cells (IgD^-IgM^+) and mature B cells (IgD^+IgM^+) (*Nr2f6*$^{+/+}$ n=3; *Nr2f6*$^{-/-}$ n=3). Means are shown; error bars represent standard error.

Figure S6: Spleenomegaly in *Nr2f6*$^{-/-}$ mice

12 month-old *Nr2f6*$^{-/-}$ mice displayed enlarged spleens with increased lymphocyte numbers in *Nr2f6*$^{-/-}$ mice.

Figure S7: Serum immunoglobin levels of aged *Nr2f6*$^{-/-}$ mice

Serum immunoglobulin levels of IgM, IgE, IgG2a and IgG2b of young (6-10 weeks) and old (>12 month) *Nr2f6*$^{-/-}$ mice were determined via ELISA. Means are shown; error bars represent standard error.

Figure S8: Reduced apoptosis response in *Nr2f6*$^{-/-}$ CD4^{+} T and B cells

(A) CD4^{+} T cells of *Nr2f6*$^{-/-}$ have a lower apoptosis rate when induced with different concentrations of anti-CD3. (B) In contrast, apoptotic rates of CD8^{+} T cells were comparable to wild-type controls. (C) Spontaneous and (D) IgM-induced B cell apoptosis rate is also significant lower when compared to wild-type controls. (A) Factorial split plot with the factors "genotypes", with the four CD3 concentrations of each cell assembly of each animal revealed a significantly difference p=0.025 (*Nr2f6*$^{+/+}$ n=6; *Nr2f6*$^{-/-}$ n=6), that could not be found in the CD8^{+} T cells. *Nr2f6*$^{-/-}$ B cells *Nr2f6*$^{+/+}$ n=6; *Nr2f6*$^{-/-}$ n=6 have a lower spontaneous (C) p=0.036, (D) and induced apoptosis rate p=0.012. Means are shown; error bars represent standard error.

Figure S9: *Nr2f6*$^{-/-}$ mice have hyper-reactive T lymphocytes

(A&B) Proliferative responses of *Nr2f6*$^{+/+}$ (n =3) and *Nr2f6*$^{-/-}$ (n =3) CD4^{+} and CD8^{+} T cells were higher in the *Nr2f6*$^{-/-}$ CD4^{+} (although not on a significant level) but not in the CD8^{+} subset. (C) IFN-γ cytokine secretion response of *Nr2f6*$^{-/-}$ CD8^{+} T cells was upregulated - although not on a significant level - upon the indicated stimuli measured by Bioplex technology. Data show the mean of three independent experiments done in duplicates; error bars represent standard error.

Figure S10: *Nr2f6*$^{-/-}$ mice have hyper-reactive B cells

Purified *Nr2f6*$^{-/-}$ splenic B cells stimulated with anti-IgM antibodies (1,2 μg/ml) plus IL-4 (25 U/ml) for 72 h showed a significant higher proliferation response than *Nr2f6*$^{+/+}$ controls. (Unpaired t-test: *Nr2f6*$^{+/+}$ n=3; *Nr2f6*$^{-/-}$ n=3; p=0.013). Data show the mean of three independent experiments; error bars represent standard error.

Figure S11: NR2F6 overexpression suppresses IL-2 secretion in CD4$^+$ T cells

(A) NR2F6 wild-type plasmid transfections of CD4$^+$ T cells suppresses IL-2 secretion of CD3/CD28 stimulated cells after 24 h. One representative experiment out of two is shown.

(B) qRT-PCR of *Nr2f6* was used to control the transfection rate and data were normalized to GAPDH.

Figure S12: siRNA-mediated knock down abrogates target *Nr2f6* mRNA levels

qRT-PCR analysis of *Nr2f6* mRNA level revealed that target *Nr2f6* mRNA expression was diminished by >90% in *Nr2f6* siRNA but not in the control siRNA bulk transfected CD4$^+$ T cells. One of two representative experiments is shown.

Figure S13: CD3 and TCR-Vβ8 surface expression on *Nr2f6*$^{-/-}$ CD3$^+$ T cells

(A) CD3 and (B) TCR-Vβ8 surface expression on T cells was comparable between *Nr2f6*$^{+/+}$ and *Nr2f6*$^{-/-}$ T cells, as shown by flow cytometry. One representative experiment out of three is shown (± SD).

Figure S14: IL-17 secretion in Th17 wild-type and *Nr2f6*-deficient cells

(A) Naïve CD4$^+$ T cells from *Nr2f6*$^{+/+}$ or *Nr2f6*$^{-/-}$ mice were differentiated under neutral (Medium) or stimulating (CD3 plus CD28) Th17 conditions for 4 days. IL-17 expressing cells were measured by intracellular staining after a 5 h PDBu plus Ionomycin pulse in the presence of Golgi-plug. One representative experiment out of three is shown. These single-cell level measurements of IL-17 expression in Th17 cells by flow cytometry confirmed data of secreted IL-17 cytokine levels obtained by BioPlex multi-analyte technology (Fig. 4G and S14B). (B) In the Th17 subset, NR2F6 function appeared specific to the effector/memory but not regulatory cells, since no effect of *Nr2f6* deficiency on IL-10 expression levels was observed. IL-10 secretion of the regulatory Th17 subsets was the same in wild-type (white

bars) and *Nr2f6*-deficient (black bars) Th17 cells. Th17 differentiation status was controlled by IL-2, IL-17 and IFN-γ secretion responses. One representative experiment of two is shown.

Figure S15: NF-AT translocation is unaltered by NR2F6

NF-ATc translocation into the nucleus in unstimulated (-) and CD3 plus CD28 stimulated (+) (A) mouse wild-type and *Nr2f6*-deficient $CD4^+$ T cells as well as in (B) Jurkat cells transfected with NR2F6-ER plasmid (under OHT co-treatment) was neither changed between the different genotypes nor between different transfected Jurkat extracts. DNA polymerase was used as loading control. One representative experiment out of 3 is shown.

Figure S16: Subsets in EAE-diseased mice did not differ between genotypes

No significant difference was seen in $Nr2f6^{-/-}$ (black bars) T and B cell subsets derived from EAE-diseased mice when compared to $Nr2f6^{+/+}$ (white bars) controls. This includes the numbers and ratios of both Treg ($FOXP3^+$) and Th17 ($IL\text{-}23R^+$) T cell effector lineages; ($Nr2f6^{+/+}$ n=5; $Nr2f6^{-/-}$ n=5). Data show the mean, error bars represent standard error.

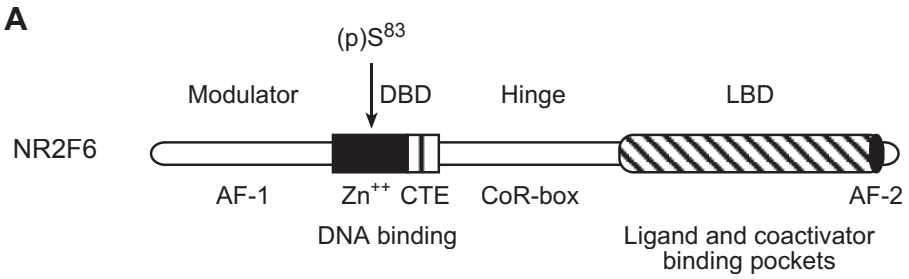
A
(p)S83
Modulator
DBD
Hinge
LBD
NR2F6
AF-1
Zn++ CTE
CoR-box
AF-2
DNA binding
Ligand and coactivator binding pockets

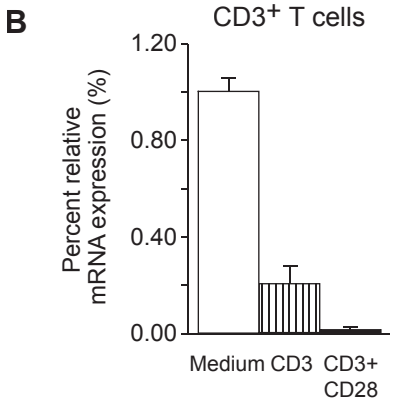
B
CD3+ T cells
Percent relative mRNA expression (%)
1.20
0.80
0.40
0.00
Medium
CD3
CD3+ CD28

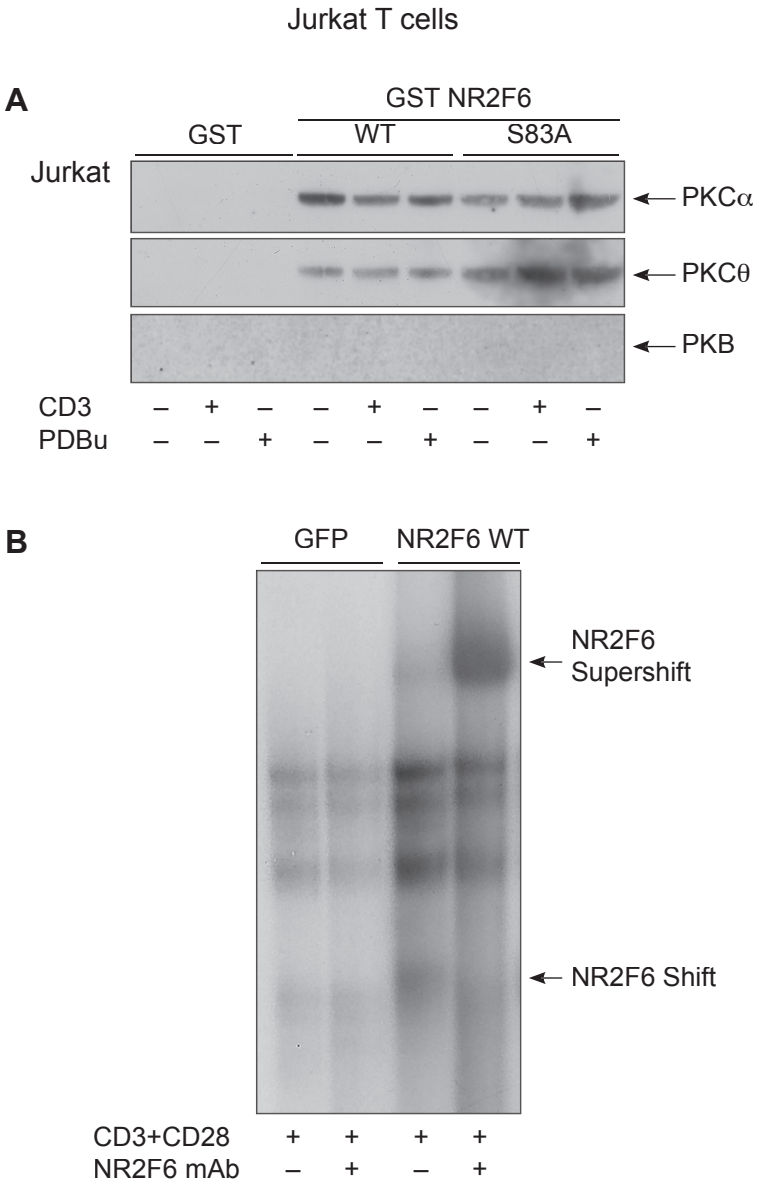
Jurkat T cells
A
GST NR2F6
GST
WT
S83A
Jurkat
PKCα
PKCθ
PKB
CD3 – + – – + – – + –
PDBu – – + – – + – – +
B
GFP
NR2F6 WT
NR2F6 Supershift
NR2F6 Shift
CD3+CD28 + + + +
NR2F6 mAb – + – +

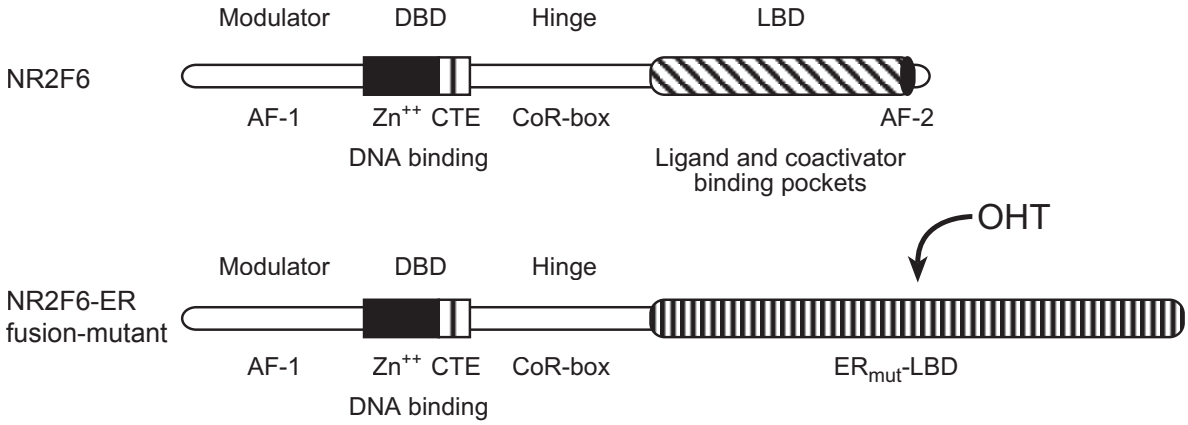
Modulator
DBD
Hinge
LBD
NR2F6
AF-1
Zn++ CTE
CoR-box
AF-2
DNA binding
Ligand and coactivator binding pockets
OHT
Modulator
DBD
Hinge
NR2F6-ER fusion-mutant
AF-1
Zn++ CTE
CoR-box
ERmut-LBD
DNA binding

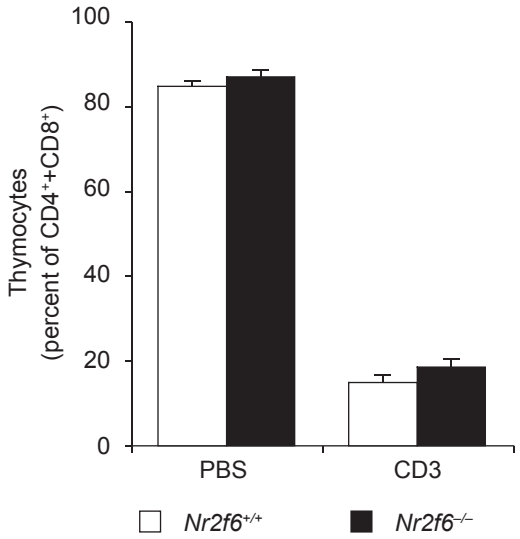
100
80
60
40
20
0
Thymocytes
(percent of CD4+CD8+)
PBS
CD3
Nr2f6+/+
Nr2f6−/−

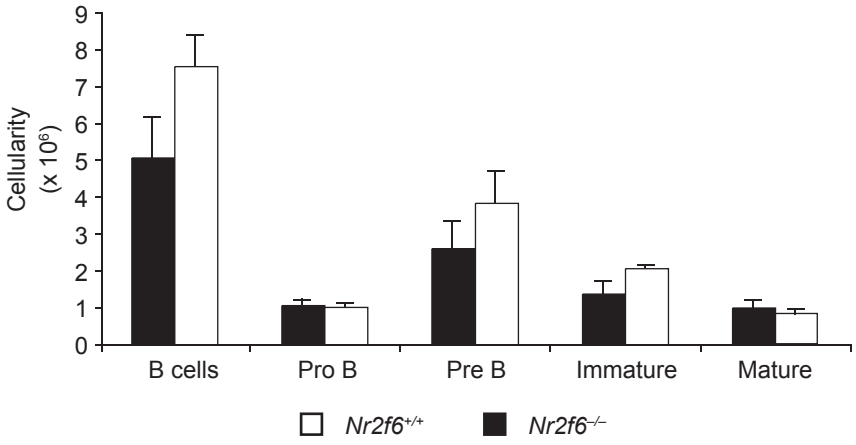
Cellularity
(x 10⁶)
9
8
7
6
5
4
3
2
1
0
B cells
Pro B
Pre B
Immature
Mature
Nr2f6+/+
Nr2f6−/−

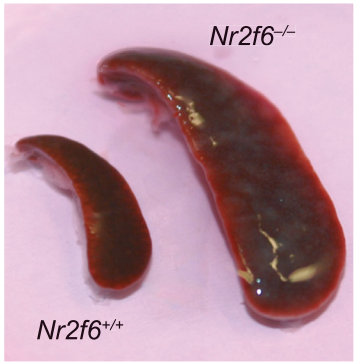
Nr2f6−/−
Nr2f6+/+

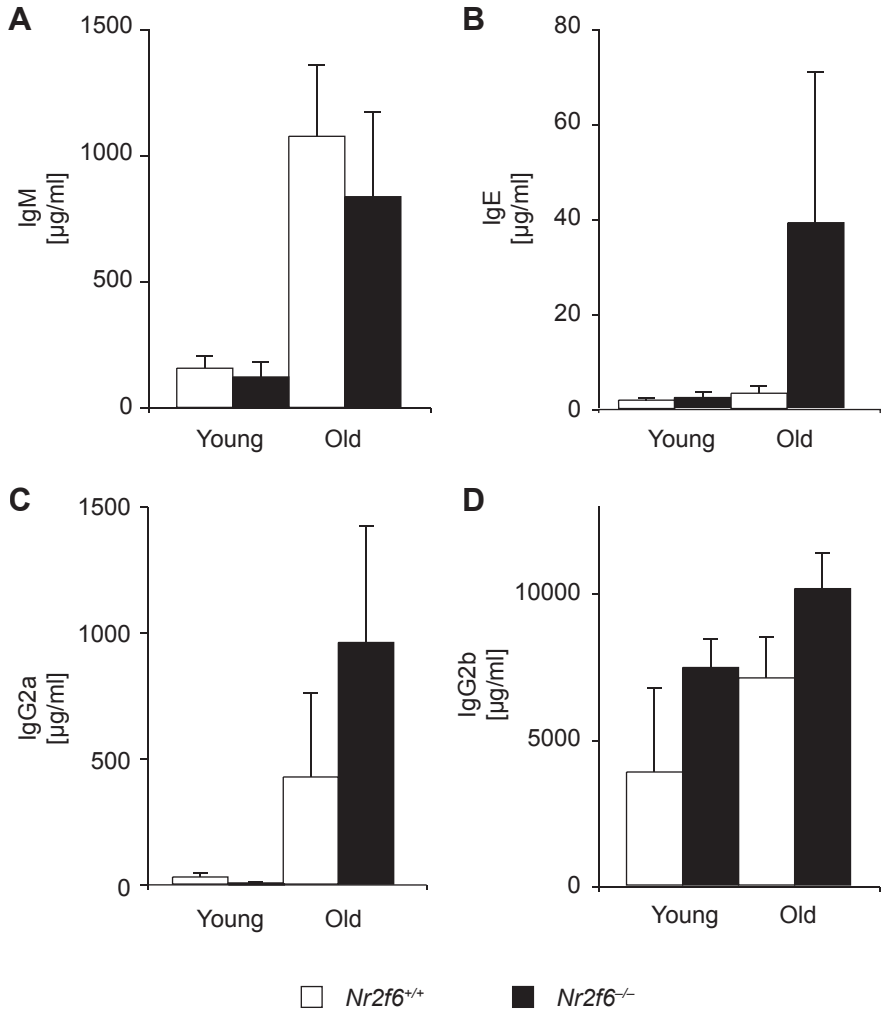
A
1500
1000
500
0
IgM [µg/ml]
Young
Old
B
80
60
40
20
0
IgE [µg/ml]
Young
Old
C
1500
1000
500
0
IgG2a [µg/ml]
Young
Old
D
10000
5000
0
IgG2b [µg/ml]
Young
Old
Nr2f6+/+
Nr2f6−/−

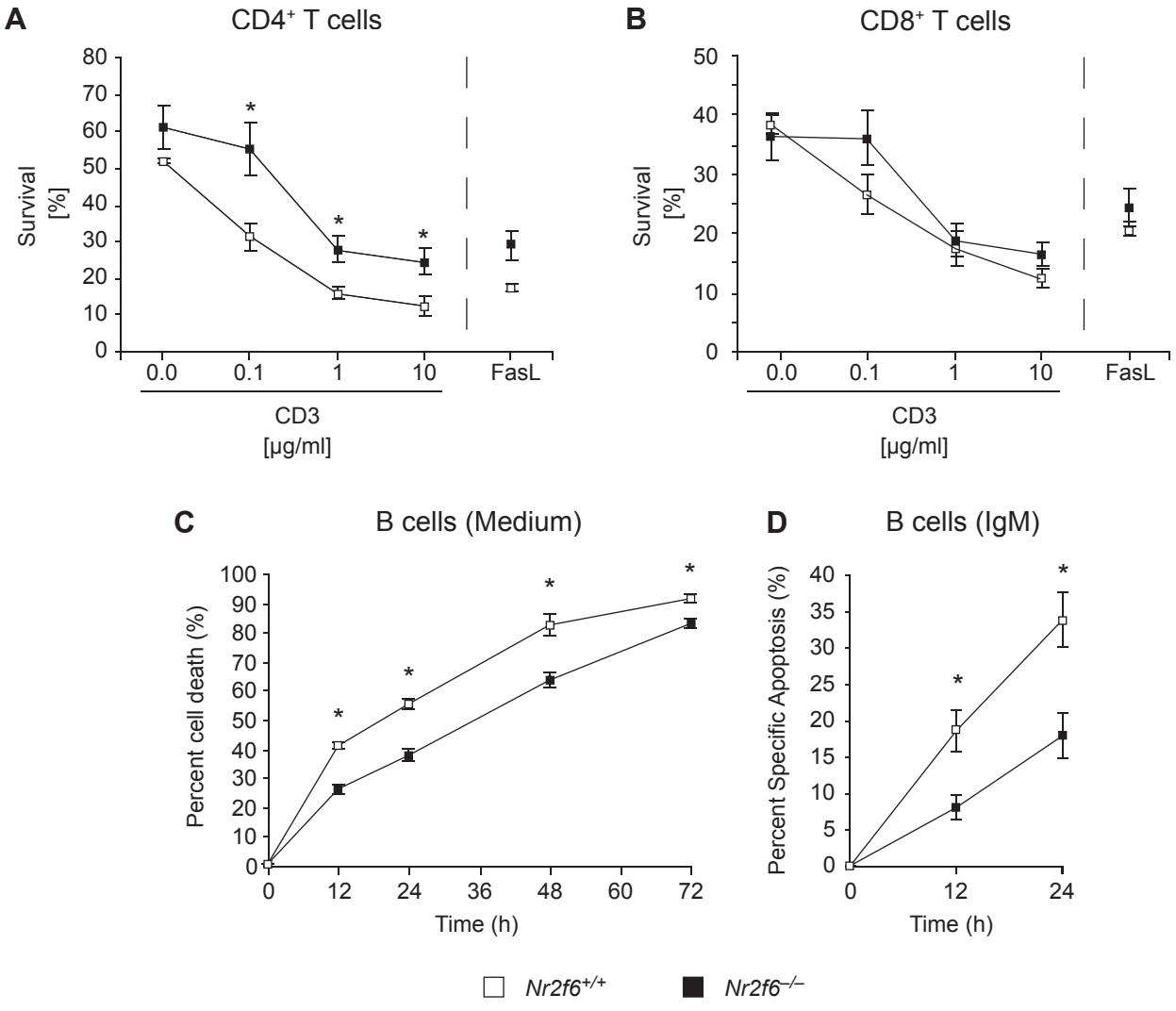
A
CD4+ T cells
Survival [%]
CD3 [µg/ml]
0.0
0.1
1
10
FasL
B
CD8+ T cells
C
B cells (Medium)
Percent cell death (%)
Time (h)
D
B cells (IgM)
Percent Specific Apoptosis (%)
Nr2f6+/+
Nr2f6−/−

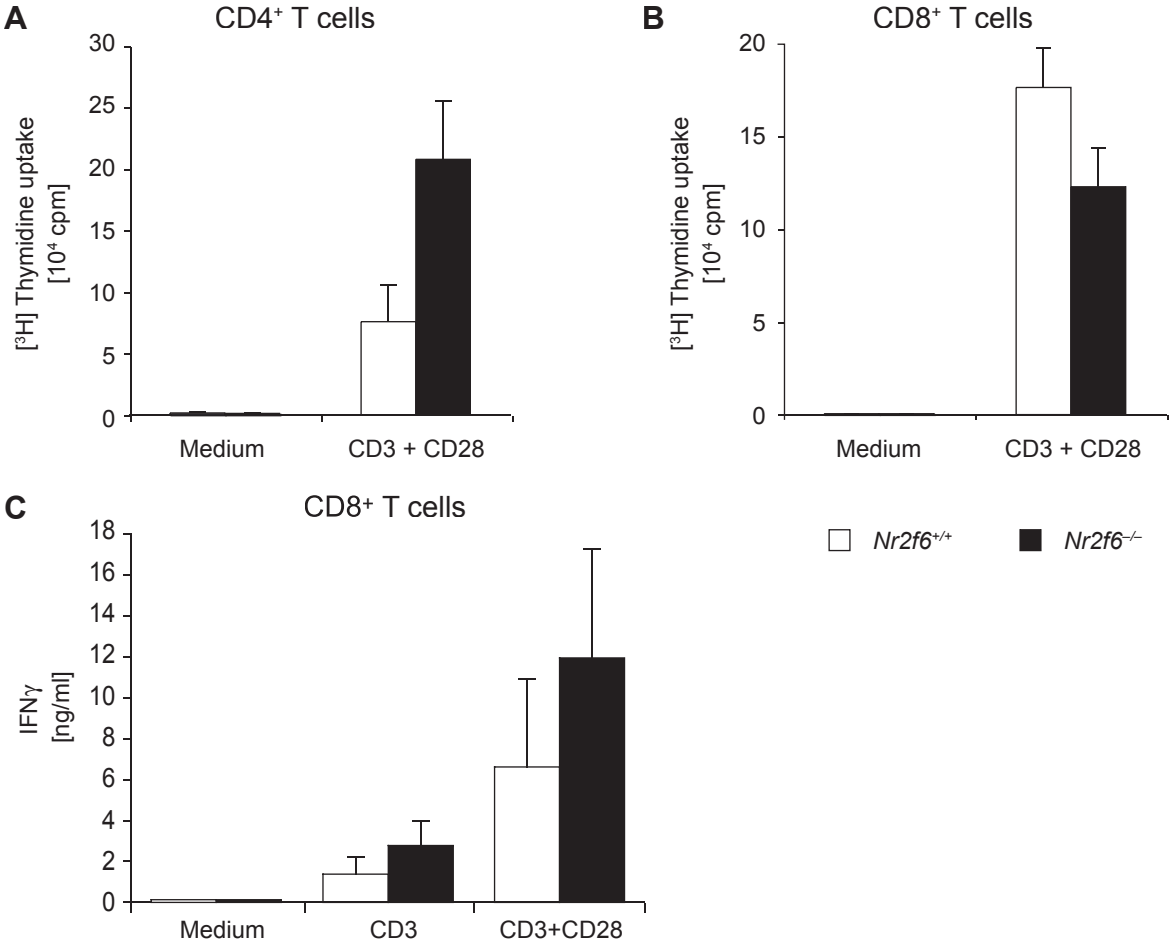
A
CD4+ T cells
[3H] Thymidine uptake [10⁴ cpm]
30
25
20
15
10
5
0
Medium
CD3 + CD28
B
CD8+ T cells
[3H] Thymidine uptake [10⁴ cpm]
20
15
10
5
0
Medium
CD3 + CD28
Nr2f6+/+
Nr2f6−/−
C
CD8+ T cells
IFNγ [ng/ml]
18
16
14
12
10
8
6
4
2
0
Medium
CD3
CD3+CD28

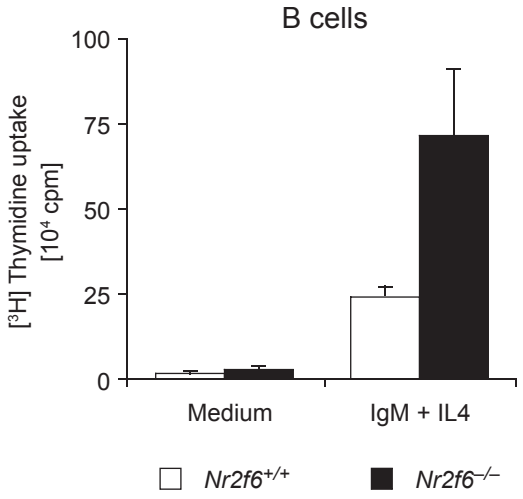
B cells
100
75
50
25
0
[3H] Thymidine uptake
[10^4 cpm]
Medium
IgM + IL4
Nr2f6+/+
Nr2f6–/–

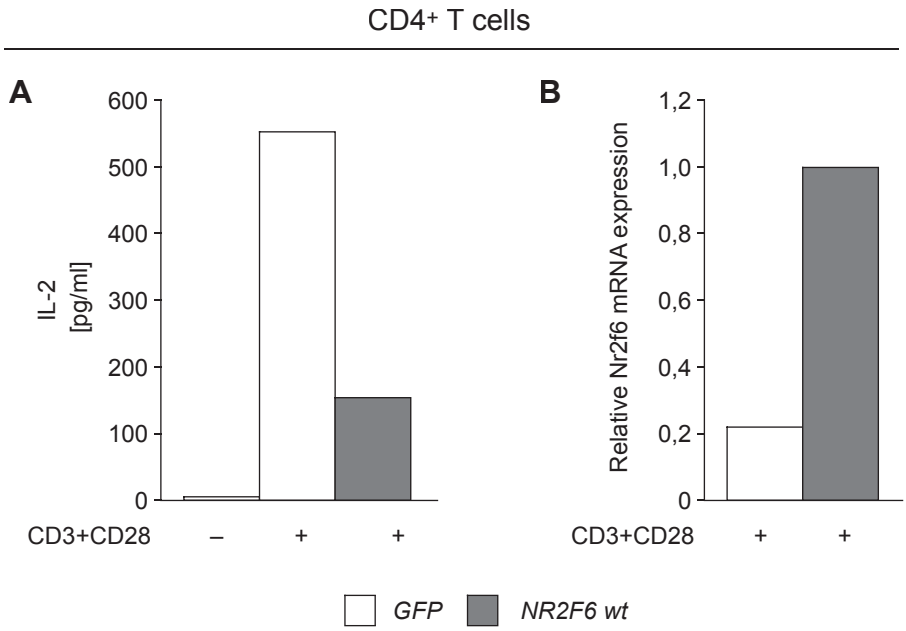
CD4+ T cells
A
IL-2 [pg/ml]
600
500
400
300
200
100
0
CD3+CD28
–
+
+
B
Relative Nr2f6 mRNA expression
1,2
1,0
0,8
0,6
0,4
0,2
0
CD3+CD28
+
+
GFP
NR2F6 wt

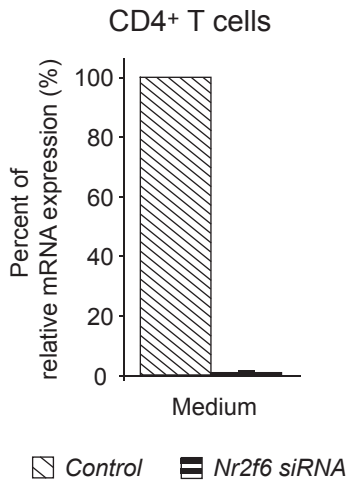
CD4+ T cells
Percent of relative mRNA expression (%)
100
80
60
40
20
0
Medium
Control
Nr2f6 siRNA

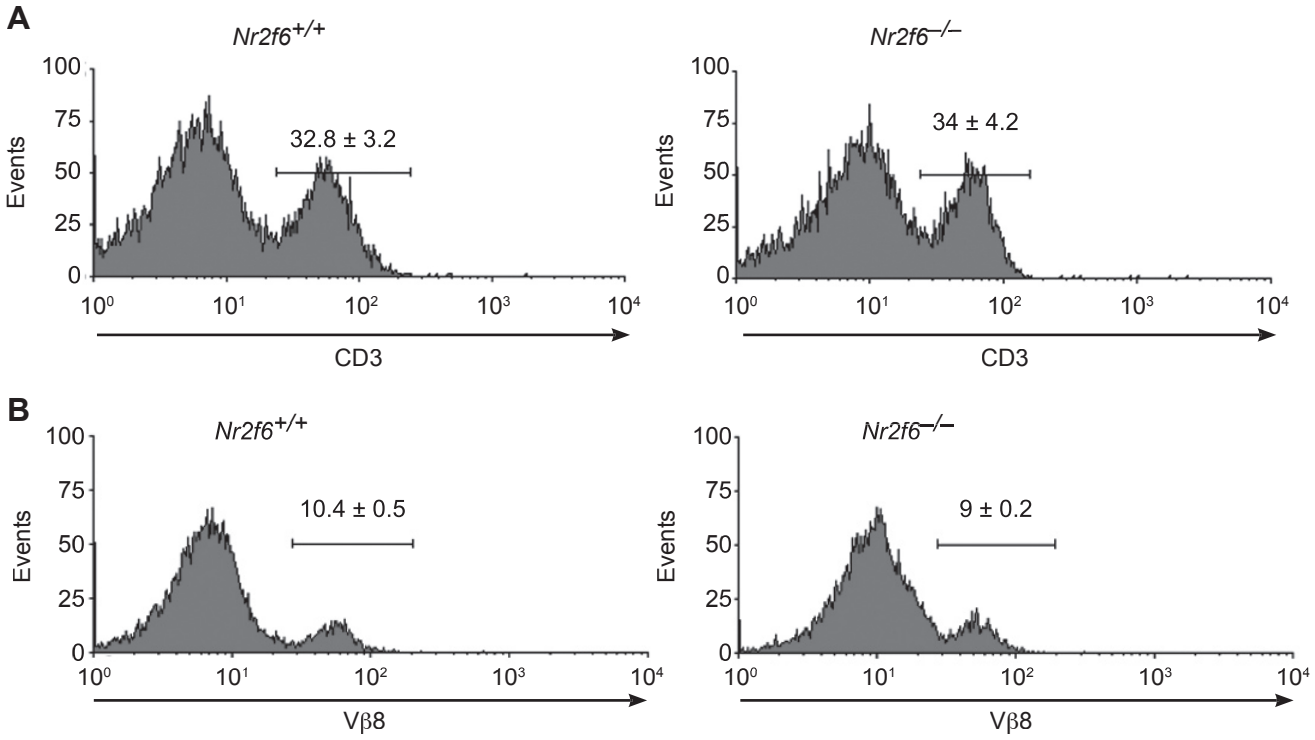
A
Nr2f6+/+
Events
100
75
50
25
0
32.8 ± 3.2
10⁰ 10¹ 10² 10³ 10⁴
CD3
Nr2f6−/−
34 ± 4.2
B
Nr2f6+/+
10.4 ± 0.5
Vβ8
Nr2f6−/−
9 ± 0.2

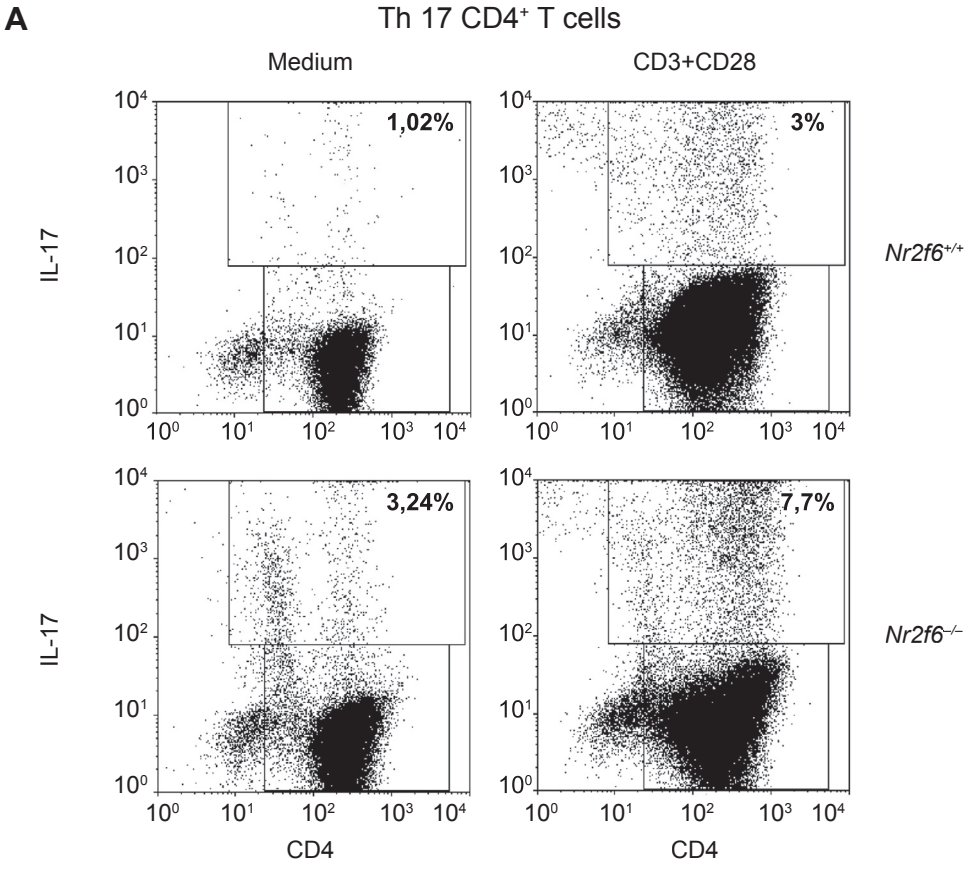
A
Th 17 CD4+ T cells
Medium
CD3+CD28
1,02%
3%
3,24%
7,7%
IL-17
CD4
Nr2f6+/+
Nr2f6−/−

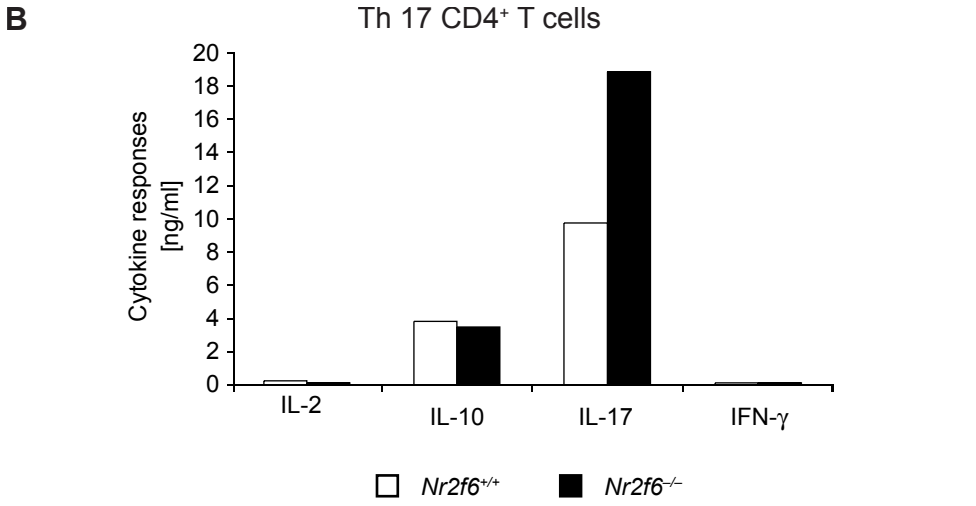
B
Th 17 CD4+ T cells
Cytokine responses [ng/ml]
IL-2
IL-10
IL-17
IFN-γ
Nr2f6+/+
Nr2f6−/−

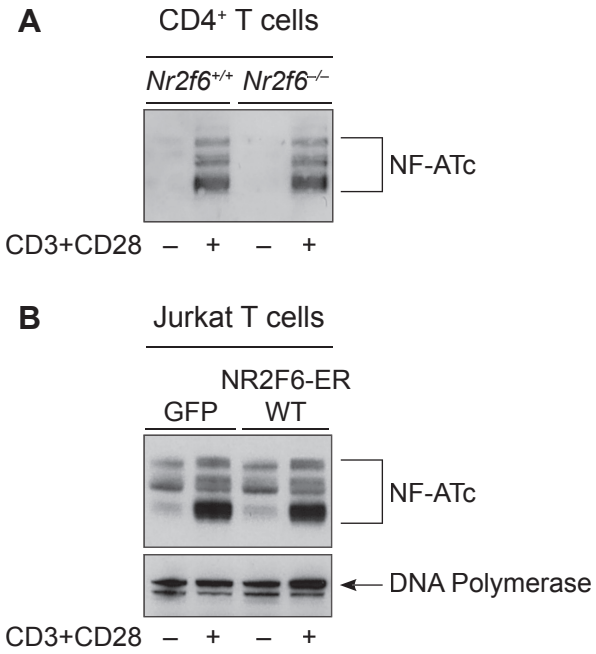
A
CD4+ T cells
Nr2f6+/+
Nr2f6–/–
NF-ATc
CD3+CD28 – + – +
B
Jurkat T cells
NR2F6-ER
GFP
WT
NF-ATc
DNA Polymerase
CD3+CD28 – + – +

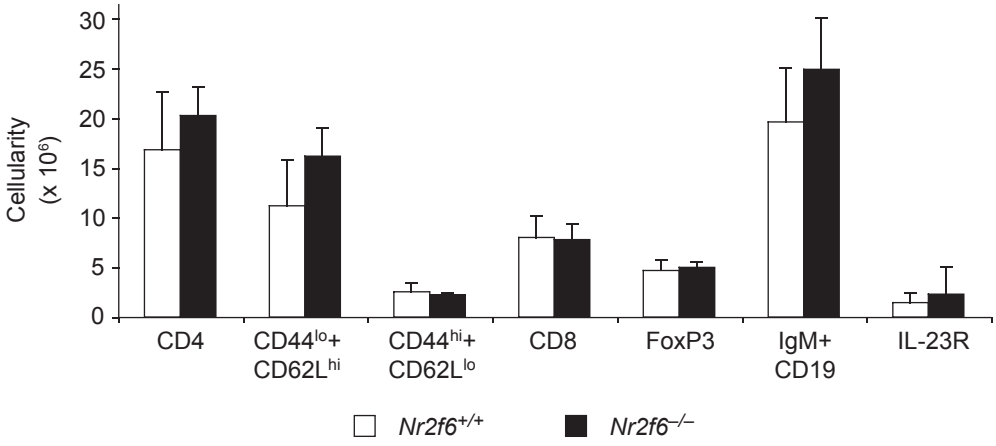
Cellularity
(x 10⁶)
30
25
20
15
10
5
0
CD4
CD44lo+
CD62Lhi
CD44hi+
CD62Llo
CD8
FoxP3
IgM+
CD19
IL-23R
Nr2f6+/+
Nr2f6−/−